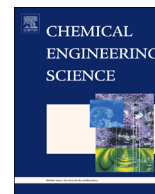




ELSEVIER

Contents lists available at ScienceDirect

## Chemical Engineering Science

journal homepage: [www.elsevier.com/locate/ces](http://www.elsevier.com/locate/ces)

# Electropolymerized polyaniline: A promising hole selective contact in organic photoelectrochemical cells

Eya Belarbi <sup>a,b</sup>, Vicente M. Blas-Ferrando <sup>a</sup>, Marta Haro <sup>a</sup>, Hager Maghraoui-Meherzi <sup>b</sup>, Sixto Gimenez <sup>a,\*</sup>

<sup>a</sup> Institute of Advanced Materials (INAM), Universitat Jaume I, 12071 Castelló, Spain

<sup>b</sup> Université de Tunis El-Manar, Faculté des Sciences de Tunis, Laboratoire de Chimie Analytique et d'électrochimie LR99ES15, Campus Universitaire de Tunis El-Manar, 2092 Tunis, Tunisia

## HIGHLIGHTS

- PANI films were processed with a systematic modification of the processing conditions.
- The structural, optical and photoelectrochemical properties of the films are reported.
- Optimized PANI films constitute promising hole selective contacts for OPECs.
- Photocurrents  $> 2 \text{ mA cm}^{-2}$  at  $-0.5 \text{ V}$  vs RHE for hydrogen generation are reported.
- Further stabilization strategies should be employed.

## ARTICLE INFO

## Article history:

Received 23 February 2016

Received in revised form

16 May 2016

Accepted 21 June 2016

## Keywords:

Polyaniline

Electropolymerization

Photoelectrochemical cell

Solar fuels

## ABSTRACT

In the present study, we have prepared Polyaniline (PANI) thin films by electrochemical polymerization on ITO substrates in acidic medium at room temperature. We have followed a systematic modification of both the precursor concentration as well as the number of electropolymerization cycles in order to optimize the response of the films as hole selective contacts for organic photoelectrochemical cells. We report the structural, optical and electrochemical properties of the PANI films aiming at providing such optimized hole selective contacts. Our results clearly confirm that PANI acts as efficient hole selective layer in these devices, with photocurrents of more than  $2 \text{ mA cm}^{-2}$  at  $-0.5 \text{ V}$  vs RHE, and  $0.3 \text{ mA cm}^{-2}$  at  $0 \text{ V}$  vs RHE for hydrogen generation and further modifications should be focused on enhancing the device stability for technological application.

© 2016 Elsevier Ltd. All rights reserved.

## 1. Introduction

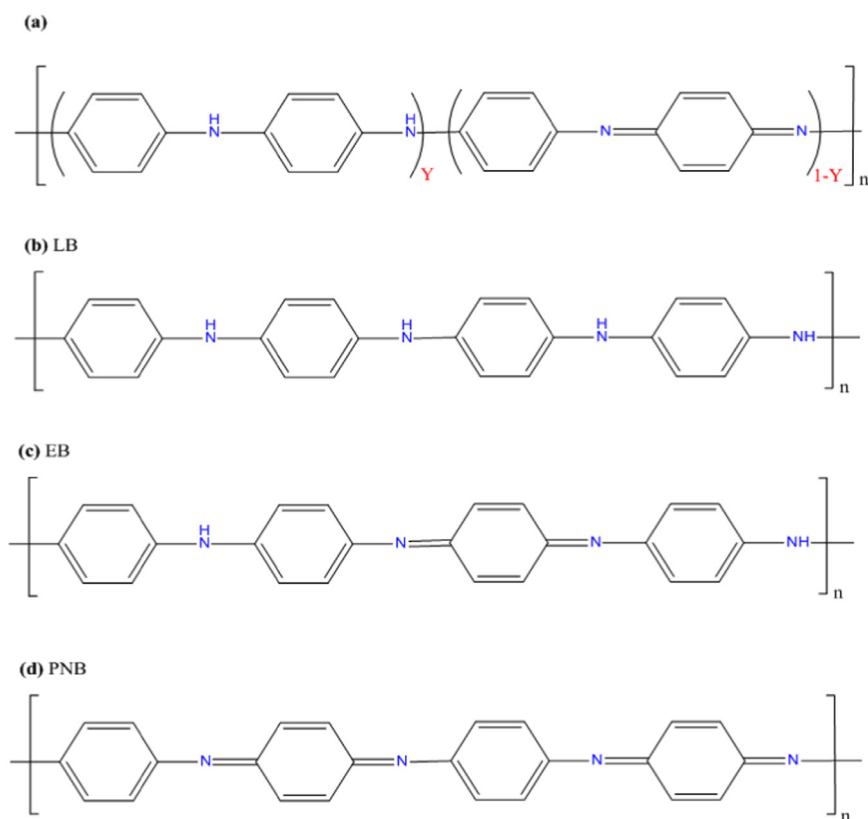
Electrically conducting polymers (ECPs) such as, Polyaniline (PANI), Polypyrrole (PPY), Polythiophene (PTh), Poly(3,4-ethylenedioxythiophene) (PEDOT) etc..., have attracted a great attention for the last two decades due to their interesting semiconducting properties. Among them, polyaniline (PANI) is one of the most promising candidates as p-type semiconductor due to its excellent environmental stability, ease of synthesis on different substrates, low cost of the monomer (Obaid et al., 2014; Sai-Anand et al., 2015), high absorption coefficient in the visible part and interesting optical, electrochemical and electrical properties (Reda and Al-Ghannam, 2012; Yusairie et al., 2012). Consequently, this

material has been widely studied for different applications in many domains such as electrochromic devices, rechargeable batteries, protection of metals against corrosion (Chaudhari and Patil, 2011; Subathira and Meyyappan, 2010), organic light emitting diodes (OLEDs) (Bejbouj et al., 2010; Park et al., 2015), organic photovoltaic cells (OPVs) (Han et al., 2014) and dye-sensitized solar cells (DSSCs) (Duan et al., 2015; Sonmezoglu et al., 2012; Taş et al., 2016).

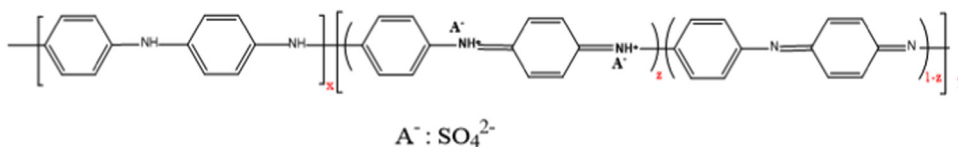
Its reversible redox chemistry allows PANI to have mainly three distinguishable oxidation states. Its most common structure is presented as Scheme 1a, where Y, ( $0 \leq Y \leq 1$ ), corresponds to the ratio of the reduced unit and  $(1 - Y)$  corresponds to the ratio of the oxidized unit. The fully reduced form ( $Y = 1$ ) is called leucoemeraldine base (LB, Scheme 1b), the half oxidized form ( $Y = 0.5$ ) is termed emeraldine base (EB, Scheme 1c) that can easily doped to obtain the conductive emeraldine salt (ES) (Scheme 2) and the

\* Corresponding author.

E-mail address: [sjulia@uji.es](mailto:sjulia@uji.es) (S. Gimenez).



**Scheme 1.** Different oxidation states of PANI: (a) polyaniline chain, (b) leucoemeraldine base, (c) emeraldine base and (d) pernigraniline base.



**Scheme 2.** The structure of doped PANI chain.

fully oxidized form ( $Y=0$ ) is referred as pernigraniline base (PNB, Scheme 1d). The delocalized  $\pi$  bonds available in the system are responsible for the semiconducting properties. The  $\pi$  and  $\pi^*$  orbitals constitute the conduction and valence band, respectively, of PANI and its difference in energy corresponds to the band gap. This value determines both the electrical and optical properties of the semi-conducting polymer. The doped ES has also an energy band called polaron band within the band gap caused by the introduction of polarons in the structure of PANI. This band can be a discrete energy level or a continuum of energy depending on the doping and final morphology of the material (Xia et al., 1995; Bhadra et al., 2009).

In the last years, there has been an increasing interest in the study of PANI as hole selective layer in organic optoelectronic devices, particularly organic photovoltaic cells. This interest arises from the fact that this layer is not yet optimized since the material should fulfill many requirements: i) to adjust the energetic barrier between active layer and electrode (allow Ohmic contact), ii) to form a selective contact for one specific sort of carriers, iii) to determine polarity of the device, iii) to control surface properties to alter the morphology of the active layer, iv) to hidden chemical or physical reaction between electrode and active layer (i.e. improving interfacial stability), and v) to improve the optical absorption of the active layer (acting as optical spacer or introducing plasmonic effects) (Yip and Jen, 2012; Steim et al., 2010). In this context, PANI is a great candidate to fulfill many of these

requirements due to its superior stability compared to other semiconductor polymers and the tunability of the electrical properties.

Despite the large number of applications, where PANI has been tested, there are only few reports addressing the generation of fuels, taking benefit of the electrocatalytic properties of this material (Croissant et al., 1998; Mascaro et al., 2004). Another interesting approach, which has been exploited in the last few years, relates to the production of solar fuels with organic photoelectrochemical cells (OPECs). Compared to inorganic devices, usually synthesized by means of high vacuum/high temperature conditions, these devices take full advantage of the versatility and potential of organic semiconductor materials to provide a real low-cost alternative for the generation of solar fuels (Esiner et al., 2013; Haro et al., 2015; Thompson and Frechet, 2008). These devices consist of an organic semiconductor material with excellent light harvesting efficiency (in general a P3HT:PCBM bulk heterojunction film is employed) sandwiched by proper selective contacts, compatible with the relevant electrochemical potentials in order to carry out the desired reactions at the semiconductor/solution interface. The main approach to provide efficient and robust devices involves the optimization of hole and electron selective contacts to deliver maximum photocurrents, but also long-term stability for real life application. The target of this study is to take advantage of the excellent p-type semiconducting properties of PANI to develop a hole selective layer for cost-effective OPEC. Furthermore, PANI

can be obtained by electrochemical polymerization, which provides an excellent control of the film thickness (by in-situ monitoring the charged passed with the potentiostat) and reduces pollution problems. Here, the method of aniline electro-oxidation by continuous cycling between two potentials was used, which provides a firmly adhered film on the electrode surface and furthermore, the film can be reduced or oxidized to control its conductivity. The final goal is optimizing a synthetic route to provide an excellent, low-cost hole selective contact, which can be easily synthesized in any laboratory and implemented as hole selective contact in organic photoelectrochemical devices. All in all, this study contributes in the advance of all-solution processable devices for the photoelectrochemical production of solar fuels.

## 2. Materials and experimental method

### 2.1. Materials

For the preparation of the PANI layers, aniline monomer (Aldrich, 99.5%) freshly distilled was used. The following reagents were used for the preparation of the electrolytic solutions, H<sub>2</sub>SO<sub>4</sub> (Sigma-Aldrich, 95–98%) and Na<sub>2</sub>SO<sub>4</sub> (Aldrich, 98%) which were solved in double-distilled water.

The organic active layer was prepared with P3HT (Luminescence Technology Corp.) and PC60BM (Solenne, 99.5%). P3HT:PCBM blends were prepared from dry *o*-dichlorobenzene (1:1, 34 mg/ml) and were stirred at 70 °C for 16 h before sample preparation. For TiO<sub>x</sub> layer were used titanium isopropoxide (Aldrich, 97%), ethanol (Panreac PA, absolut), isopropanol (Aldrich, 99.5%), and hydrochloric acid (Sigma-Aldrich, 37%). For the preparation of the electrolytic solutions, Na<sub>2</sub>SO<sub>4</sub> (Aldrich, 98.0%) and H<sub>2</sub>SO<sub>4</sub> (Fluka, 99.0%) were solved in milli-Q double-distilled water.

### 2.2. Electropolymerization of the PANI layer

All the electrochemical measurements were performed, with a PGSTAT-30 Autolab potentiostat, in a single compartment of three electrode cells on ITO substrates as working electrode and platinum and an Ag/AgCl (KCl, 3 M) as a counter electrode and a reference electrode, respectively. Polyaniline was electropolymerized from aqueous solution containing different concentrations of the monomer (10<sup>-2</sup>, 2 · 10<sup>-2</sup> and 4 · 10<sup>-2</sup> M) and H<sub>2</sub>SO<sub>4</sub> (0.1 M) as electrolytic medium with different number of cycles (4, 5, 6, 8 and 10 cycles) in a potential range between -0.2 V and 1.2 V vs the Ag/AgCl electrode, applying a scan rate of 20 mV/s.

### 2.3. Assembly of organic photoelectrochemical (OPEC) devices

Organic photocathodes were prepared in the configuration ITO/PANI/P3HT:PC60BM/TiO<sub>x</sub>/Pt. The ITO/PANI electropolymerized layers were employed as hole selective contact. Then, the P3HT:PCBM blend was deposited on top of PANI at 1200 rpm for 60 s, and the sample was introduced in a Petri dish and was allowed to dry over a period of 2 h. After this time the active layer was thermally treated at 130 °C for 10 min. The device is taken outside the glovebox. The TiO<sub>x</sub> solution (Haro et al., 2015) was filtered through a nylon filter (0.45 μm pore size) and was spin-coated on the active layer in air at 1000 rpm for 60 s and kept in the ambient at room temperature for 2 h. A thermal treatment at 85 °C for 10 min was observed to be beneficial for the device performance. Thin platinum layer was sputtered by using a BALTEC (SCD 500) sputter coater by using a current of 50 mA for 2–5 s while keeping the distance between Pt source and substrates at ~5 cm at a base pressure of 5 × 10<sup>-3</sup> mbar. This provides a Pt thickness of ~0.5 nm according to the calibration curve provided by the manufacturer.

### 2.4. Characterization techniques

The optical properties of the PANI layers were characterized by an UV–vis spectroscopy using a Varian Cary 300 Bio spectrophotometer. The PANI films on ITO substrates and produced OPEC devices were characterized by a JEOL JEM-3100F field emission scanning electron microscope (FEG-SEM). Photoelectrochemical characterization of the OPEC devices was performed in a three-electrode configuration, where a graphite bar and an Ag/AgCl (KCl, 3 M) were, respectively, used as counterelectrode and as reference. The electrolyte was Na<sub>2</sub>SO<sub>4</sub> 0.1 M and we added to the solution H<sub>2</sub>SO<sub>4</sub> until pH 2 was reached. The area of the electrodes was 0.5 cm<sup>2</sup>. The electrodes were illuminated directly to the substrate while the electrode is in contact to the electrolyte using a 300 W Xe lamp. The light intensity was adjusted to 100 mW cm<sup>-2</sup> using an optical power meter 70310 from Oriel Instruments where a Si photodiode was used to calibrate the system. All potentials have been referred to the RHE electrode:  $E_{\text{RHE}} = E_{\text{Ag/AgCl}} + 0.210 + 0.059 \cdot \text{pH}$ . Linear sweep voltammetry (5 mV/s) and chronamperometric measurements (stability tests) were performed with a PGSTAT-30 Autolab potentiostat under chopped light. Electrochemical impedance spectroscopy (EIS) measurements of the PANI layer were performed in a 0.1 M Na<sub>2</sub>SO<sub>4</sub> solution, acidified to pH 2 with H<sub>2</sub>SO<sub>4</sub>, using the Autolab apparatus under illumination conditions.

## 3. Results and discussion

### 3.1. Electrochemical polymerization of PANI

As mentioned before, the only conductive form of PANI is emeraldine salt, which can be obtained from emeraldine base (see Scheme 1), by doping the polymer with strong acids. In our case, in order to improve the electrical properties of this polymer, the choice of a sulfuric acidic environment (0.1 M H<sub>2</sub>SO<sub>4</sub>) was dictated by the low conductivity of PANI in neutral or basic conditions. This phenomenon is due to the presence of polarons and the reduced form of PANI under these conditions (Bhadra et al., 2009; Winther-Jensen and MacFarlane, 2011). The doped PANI structure with H<sub>2</sub>SO<sub>4</sub> is shown in Scheme 2.

PANI was electropolymerized onto ITO substrates with different concentrations of the monomer and different number of electropolymerization cycles. The thickness of the as synthesized PANI layers was characterized by contact profilometry and the obtained results are compiled in Table 1. The different PANI layers are labeled as X.Y, where X denotes the number of electropolymerization cycles and Y is the concentration of the monomer (·10<sup>-2</sup> M). Unfortunately, the thickness of the samples with the lowest tested concentration (10<sup>-2</sup> M) and lowest number of electropolymerization cycles (sample 4.2) could not be properly evaluated by contact profilometer.

Further structural characterization was carried out by SEM and Fig. 1 shows the top-views of PANI layers with different processing conditions. Only samples with 10<sup>-2</sup> M and 2 · 10<sup>-2</sup> M monomer concentration were tested, since higher monomer concentration (4 · 10<sup>-2</sup> M) led to films too thick as selective contacts. In terms of morphology, there seems to be minor differences between the different layers synthesized with the same precursor concentration and as the number of electropolymerization cycles increase, the definition of the grains seems to decrease. This behavior has been explained by Guo and Zhou (2007) as “gel effect” in which one part of the oligomers is oxidized to PANI and the others converted into gel, after interaction between the dopant and aniline monomer, to form the nanofibers of PANI. With the presence of the gels, the amount of the nucleation sites decreased to favor the one dimensional growth (Wang et al., 2012).

**Table 1**

Thickness of the PANI layers electropolymerized on ITO substrates measured by contact profilometry. Sample code is X.Y, where X is the number of electropolymerization cycles and Y is the concentration of the monomer ( $\cdot 10^{-2}$  M).

Sample	Thickness (nm)
4.1	–
5.1	–
6.1	–
4.2	–
5.2	55.0
6.2	213.3
4.4	149.4
5.4	156.0
6.4	201.5

The electrochemical behavior of PANI layer was investigated by cyclic voltammetry in a potential range between  $-0.2$  V and  $1.2$  V vs the Ag/AgCl electrode, applying a scan rate of  $20$  mV/s (Fig. 2). Again, both the concentration of monomer in the solution maintaining the concentration of acid (i.e. changing monomer:doping agent ratio), and the number of electrolymerization cycles were changed.

Fig. 2(a) shows the cyclic voltammograms of the growth of PANI, on ITO electrode, from  $\text{H}_2\text{SO}_4$  aqueous acidic solution containing  $2 \cdot 10^{-2}$  M of monomer with different number of cycles (4, 5, 6, 8 and 10 cycles). The cyclic voltammetry curves showed the presence of 3 different oxidation states. The peak at around  $0.3$  V corresponds to the conversion between leucoemeraldine state (LB) and emeraldine salt state (ES), the one at  $0.5$  V refers to further oxidation and the anion doping process of PANI and the last one that appearing at  $0.9$  V corresponds to the conversion between emeraldine salt state and pernigraniline state (PNB) (Motheo et al., 1998; Wang et al., 2013). In the oxidized state, conducting polymers like PANI are charge-balanced, «doped» with counter anions ('p-doping') and have a delocalized  $\pi$ -electron band structure (Yusairie et al., 2012).

The current density increases with both the number of cycles and the concentration of monomer as shown in Fig. 2(b), which relates to the growth of the electroactive polyaniline films on the ITO substrate, directly increasing the thickness of the PANI layer during the successive cycles performed (Alonso et al., 2009), in good correlation with the information provided by Table 1. The increase of the current density can be explained by its proportionality to the concentration of the monomer as dictated by the Randles-Sevcik equation (Neghmouche and Lanez, 2013):

$$i_p = 0.4463 n F A C \left( \frac{n F s D}{RT} \right)^{1/2}$$

where  $i_p$  is the peak current,  $n$  is the number of electrons,  $F$  is Faraday constant,  $T$  is the temperature in Kelvin,  $R$  is the gas constant,  $A$  is the surface area of the working electrode,  $D$  is the diffusion coefficient of the electroactive species,  $C$  is the bulk concentration of the electroactive species (the monomer) and  $s$  is the scan rate of voltammograms.

The optical properties of different  $\text{H}_2\text{SO}_4$  doped PANI films electropolymerized under different conditions are shown in Fig. 3. In order to evaluate the effect of the monomer:dopant agent ratio on the optical properties to optimize the HSL, the UV-vis spectra of three samples obtained with solutions of different concentrations of aniline were measured. Two clear absorption bands can be observed. The band located at around  $350$  nm can probably be related to the  $\pi$ - $\pi^*$  transition centered on the benzoid rings, and a second broad band from  $500$  nm to  $700$  nm, can be assigned to the polaron/bipolaron transitions caused by the interband charge transfer from benzoid to quinoid rings confirmed the doped polyaniline state (Wang et al., 2013; Ashokan et al., 2015). On the

other hand, according to Nekrasov et al. (2000) the intense band at  $350$  nm ( $3.3$  eV) is characteristic of the protonated forms of emeraldine salt, while the large one located from  $500$  nm to  $700$  nm, which appears when the potential range of electropolymerization increases up to  $0.6$  V, is a superposition of three important bands marked at  $\sim 570$ ,  $\sim 665$  ( $1.86$  eV), and  $755$  nm. These latter bands are relative to donor-acceptor interaction between the quinoid fragments and the counter anion (which is  $\text{HSO}_4^-$  in our study), exciton transitions in quinoid rings and the localized polarons, respectively. We believe that the latter interpretation by Nekrasov et al. is more accurate, since it describes more precisely the different transition states occurring during the film growth.

As can be seen in Fig. 3, the increase of the monomer concentration increases the intensity of the absorbance band located at  $350$  nm, which is directly related to the increase of the film thickness. However, the intensity of the second band present at  $> 450$  nm decreases. This decrease may be due to the growing rate of the end product formation, which occurs after increasing the monomer concentration and leads to the continuous decrease of the amount of intermediates (Malinauskas and Holze, 1998; Zhang et al., 2011). Similar results were obtained for different numbers of electropolymerization cycles.

In order to gain further insight into the intrinsic electronic properties of the synthesized PANI films, we carried out impedance spectroscopy (IS) measurements in three-electrode configuration in an aqueous solution for different applied voltages under illumination (see Section 2). The Nyquist plots ( $-Z''$  vs  $Z'$ ) systematically showed a semicircular shape and consequently we used the basic Randles' circuit ( $R_s - R_{ct}C$ ) to fit the experimental data. The fitted resistances and capacitances are plotted in Fig. 4. The series resistance shows a factor 10 reduction when moving from 4 cycles to 5 or 6 cycles, which can be directly related to the quality of the improvement of the ITO/PANI contact (Fig. 4a). Further increase of the number of cycles to 8 and 10, leads to much higher series resistances, in the order of  $100 \Omega \text{ cm}^2$ . It is interesting to note that slightly lower series resistances are measured in the dark (not shown), compared to measurements under illumination. The charge transfer resistance of the different films increases with the number of cycles, although at the more cathodic potentials, all values seem to converge (Fig. 4b). On the other hand, the capacitance of the films (Fig. 4c) increases from 4 to 5 and 6 cycles. This behavior is consistent with the chemical capacitance of PANI and can be related to a full coverage of the ITO surface at 5 cycles. Subsequently, after 8 and 10 cycles, the capacitance seems to be dominated by the double layer capacitance (around  $10^{-5} \text{ F cm}^{-2}$ ). From these measurements, the films with 5 electropolymerization cycles seem to combine the best properties to perform as hole selective contact in photovoltaic/photoelectrochemical devices, since these conditions provide full coverage of the ITO surface with low resistance.

From the above fundamental characterization of the PANI films synthesized with different conditions, we selected the sample with  $2 \cdot 10^{-2}$  monomer concentration and different electropolymerization cycles and used these layers as hole selective contact in organic photoelectrochemical cells, with architecture ITO/PANI/P3HT:PCBM/TiO<sub>x</sub>/Pt. Due to the choice of selective contacts carried out, this device works as a photocathode driving the photogenerated electrons to the solution and the photogenerated holes to the contact. The photoelectrochemical performance of the devices under chopped illumination ( $j$ - $V$  curve) is showed as Fig. 5a. The optimum device (with 5 electropolymerization cycles) can deliver an outstanding photocurrent of more than  $2 \text{ mA cm}^{-2}$  at  $-0.5$  V vs RHE, and  $0.3 \text{ mA cm}^{-2}$  at  $0$  V vs RHE. Moreover, the obtained behavior is reproducible as showed in Fig. 5b, where the results of two identical devices are showed.

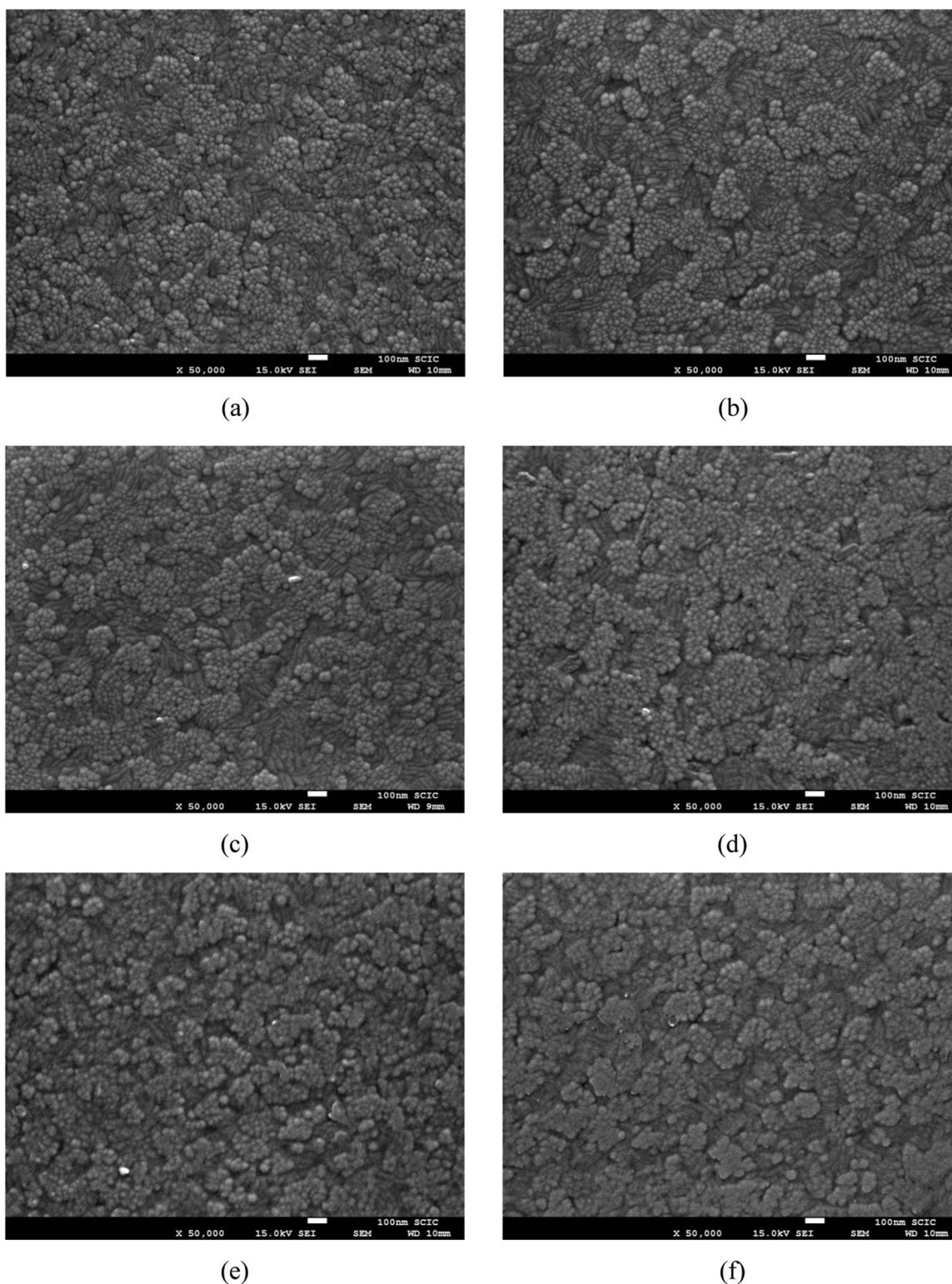


**Fig. 1.** Top view of different PANI layers on ITO substrates (a) 4.1, (b) 4.2, (c) 5.1, (d) 5.2, (e) 6.1 and (f) 6.2. Sample code is  $xy$ , where  $x$  is the number of electropolymerization cycles and  $y$  is the concentration of the monomer ( $\cdot 10^{-2}$  M).

In a recent study a direct relation between the onset potential for  $H_2$  evolution and the work function of the hole selective layer (HSL) has been demonstrated (Bourgeteau et al., 2016). In this context, the work function of PANI is around 4.5–4.8 eV depending on the doping state (Abdulrazzaq et al., 2015). Therefore, the value of the onset potential for  $H_2$  evolution around 0.1 V vs. RHE could be expected, although it can be improved until 0.3–0.4 eV. This

sets a possible limitation for this system, although we believe that it can be counterbalanced due to the advantages that the use of PANI involves, in terms of simplicity and reproducibility of the synthetic method, as well as the tunability of the optical and electrical properties. Moreover, the method proposed here allows assembling a hole selective layer to different nanostructured substrates, opening new perspectives in the design of organic

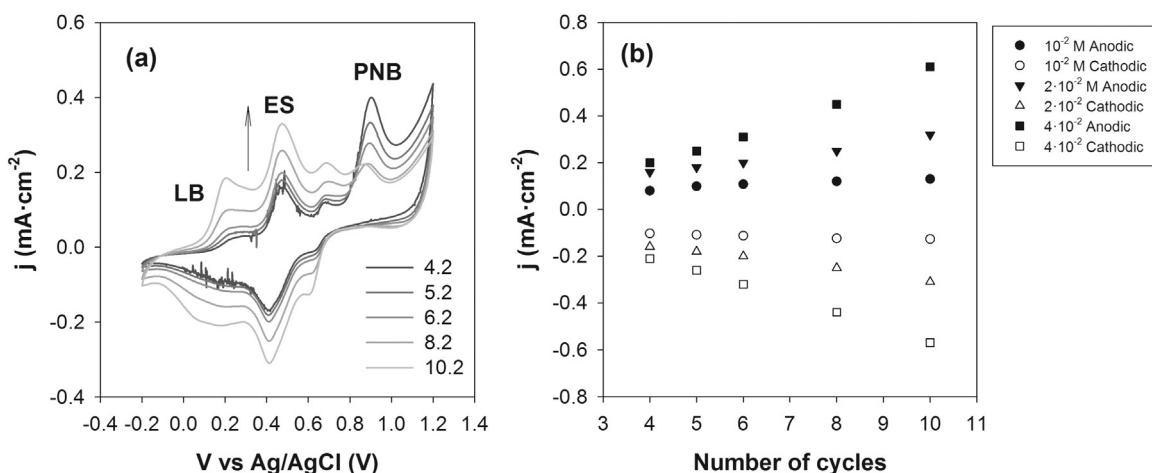


**Fig. 2.** (a) Cyclic voltammogram of PANI layer recorded in  $2 \cdot 10^{-2}$  M of aniline monomer and (b) anodic and cathodic peak density current vs sweep cycles at different concentrations of aniline monomer, in 0.1 M  $H_2SO_4$  and at a scan rate 20 mV/s.

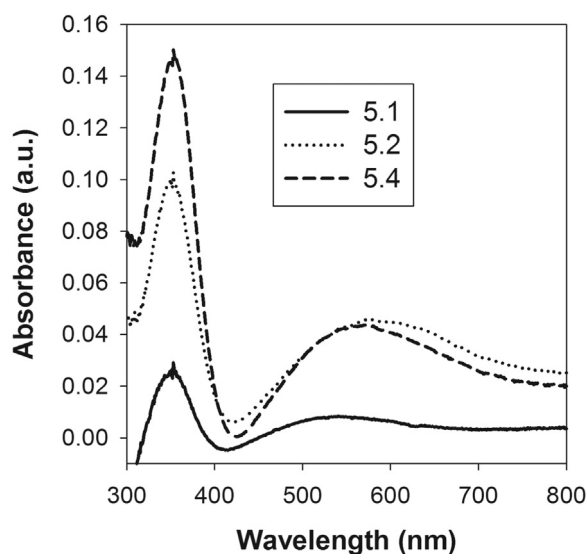


**Fig. 3.** UV-vis absorption spectra of PANI films doped  $H_2SO_4$  (0.1 M) at different concentrations of monomer and a constant number of cycles (5 cycles).

photocathodes for solar fuel production.

Finally, the stability of the device was evaluated through chronoamperometric tests at 0 V vs RHE with chopped illumination (Fig. 5c). After one hour testing, the photocurrent is decreased

70%, indicating that further stabilization strategies should be employed in order to fully exploit the capabilities of this device. Notably, after the measurements no delamination of the film is observed. The observed low stability is similar to that obtained with cross-linked PSS:PEDOT hole selective layer when the same ESL/catalyst was used (Haro et al., 2015). In that study, the stability was remarkably improved when a thicker electron selective layer was deposited, but increasing electron conductivity problems within the ESL. For this reason, the mechanisms of loss of performance and the development of protective electron selective layer are currently under investigation in our lab.

#### 4. Conclusions

Based on a systematic modification of the synthesis parameters for the electrodeposition of PANI layers, we have showed that PANI can efficiently act as hole selective layer in organic photoelectrochemical cells for hydrogen generation from proton reduction. Remarkable values of more than  $2 \text{ mA cm}^{-2}$  at  $-0.5 \text{ V}$  vs RHE, and  $0.3 \text{ mA cm}^{-2}$  at 0 V vs RHE have been obtained for the optimized device, although further modifications should be carried out in order to enhance the stability of the layers for technological application.

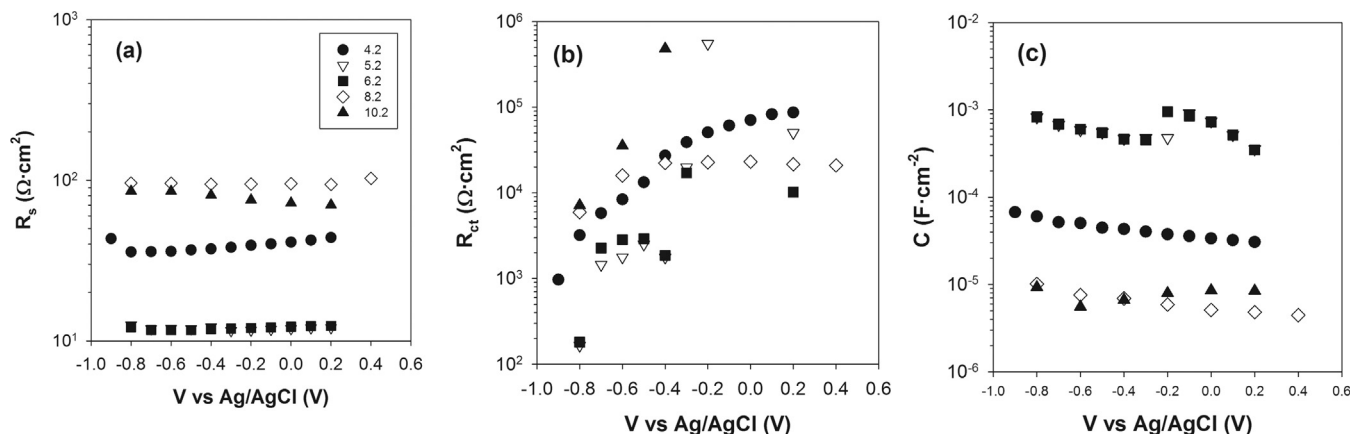


**Fig. 4.** (a) Series resistance ( $R_s$ ), (b) charge transfer resistance ( $R_{ct}$ ) and (c) capacitance (C) of the PANI films with  $2 \cdot 10^{-2}$  M precursor concentration and different numbers of electropolymerization cycles under illumination.

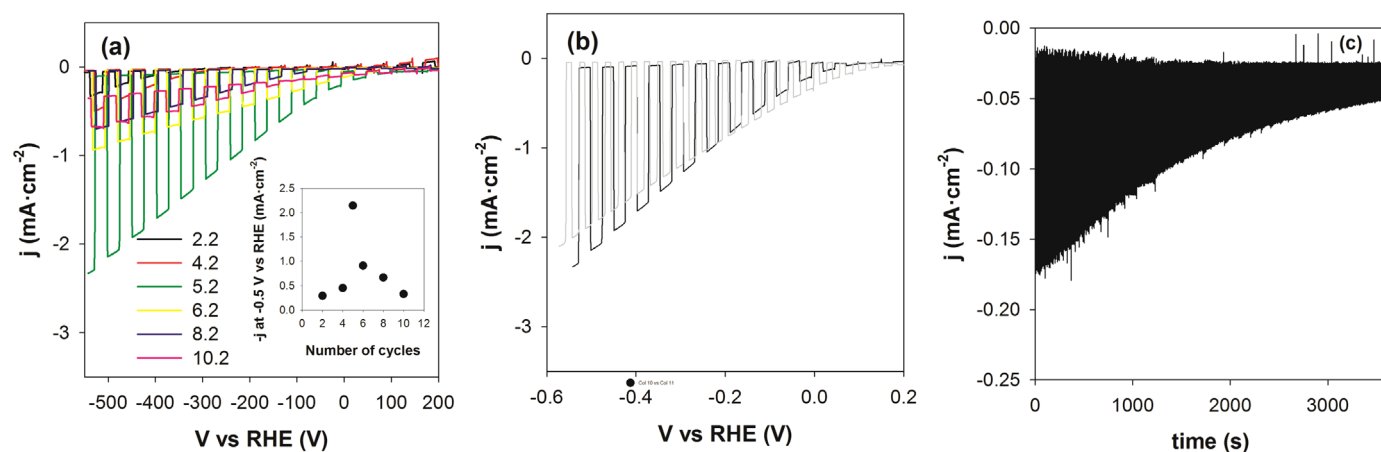


**Fig. 5.** (a)  $j$ - $V$  curves of ITO/PANI/P3HT:PCBM/TiO<sub>x</sub>/Pt devices for hydrogen generation with different PANI layers obtained with 2, 4, 5, 6, 8 and 10 electropolymerization cycles (monomer concentration  $2 \cdot 10^{-2}$  M). (b)  $j$ - $V$  curves of two identical ITO/PANI/P3HT:PCBM/TiO<sub>x</sub>/Pt devices with the optimum PANI layer (sample 5.2) and (c) Chronoamperometric test at 0 V vs RHE of a representative ITO/PANI/P3HT:PCBM/TiO<sub>x</sub>/Pt device for hydrogen generation. The PANI layer corresponds to sample 5.2.

## Acknowledgments

We thank financial support from the University Jaume I through the project P1·1B2011-50 and from the European Community through the Future and Emerging Technologies (FET) programme under the FP7, collaborative Project contract no. 309223 (PHOCS). Serveis Centrals at UJI (SCIC) are acknowledged. Authors wish to thank also the Tunisian Ministry of Higher Education and Scientific Research (MHESR) for the financial support of this work.

## References

- Abdulrazzaq, O., Bourdo, S.E., Saini, V., Watanabe, F., Barnes, B., Ghosh, A., Biris, A.S., 2015. Tuning the work function of polyaniline via camphorsulfonic acid: an X-ray photoelectron spectroscopy investigation. *RSC Adv.* 5, 33–40.
- Alonso, J.L., Ferrer, J.C., Cotarelo, M.A., Montilla, F., de Avila, S.F., 2009. Influence of the thickness of electrochemically deposited polyaniline used as hole transporting layer on the behaviour of polymer light-emitting diodes. *Thin Solid Films* 517, 2729–2735.
- Ashokan, S., Ponnuswamy, V., Jayamurugan, P., Chandrasekaran, J., Rao, Y.V.S., 2015. Influence of the counter ion on the properties of organic and inorganic acid doped polyaniline and their Schottky diodes. *Superlattices Microstruct.* 85, 282–293.
- Bejbouj, H., Vignau, L., Miane, J.L., Olinga, T., Wantz, G., Mouhsen, A., Oualim, E.M., Harmouchi, M., 2010. Influence of the nature of polyaniline-based hole-injecting layer on polymer light emitting diode performances. *Mater. Sci. Eng. B: Adv. Funct. Solid-State Mater.* 166, 185–189.
- Bhadra, S., Khastgir, D., Singha, N.K., Lee, J.H., 2009. Progress in preparation, processing and applications of polyaniline. *Prog. Polym. Sci.* 34, 783–810.
- Bourgeteau, T., Tondelier, D., Geffroy, B., Brisse, R., Campidelli, S., Cornut, R., Jous-selme, B., 2016. All solution-processed organic photocathodes with increased efficiency and stability via the tuning of the hole-extracting layer. *J. Mater. Chem. A* 4, 4831–4839.
- Chaudhari, S., Patil, P.P., 2011. Inhibition of nickel coated mild steel corrosion by electro-synthesized polyaniline coatings. *Electrochim. Acta* 56, 3049–3059.
- Croissant, M.J., Napporn, T., Leger, J.M., Lamy, C., 1998. Electrocatalytic oxidation of hydrogen at platinum-modified polyaniline electrodes. *Electrochim. Acta* 43, 2447–2457.
- Duan, Y., Chen, Y., Tang, Q., Zhao, Z., Hou, M., Li, R., He, B., Yu, L., Yang, P., Zhang, Z., 2015. A dye-sensitized solar cell having polyaniline species in each component with 3.1%-efficiency. *J. Power Sources* 284, 178–185.
- Esiner, S., van Eersel, H., Wienk, M.M., Janssen, R.A.J., 2013. Triple junction polymer solar cells for photoelectrochemical water splitting. *Adv. Mater.* 25, 2932–2936.
- Guo, Y., Zhou, Y., 2007. Polyaniline nanofibers fabricated by electrochemical polymerization: a mechanistic study. *Eur. Polym. J.* 43, 2292–2297.
- Han, Y.-K., Chang, M.-Y., Ho, K.-S., Hsieh, T.-H., Tsai, J.-L., Huang, P.-C., 2014. Electrochemically deposited nano polyaniline films as hole transporting layers in organic solar cells. *Sol. Energy Mater. Sol. Cells* 128, 198–203.
- Haro, M., Sois, C., Molina, G., Otero, L., Bisquert, J., Gimenez, S., Guerrero, A., 2015. Toward stable solar hydrogen generation using organic photoelectrochemical cells. *J. Phys. Chem. C* 119, 6488–6494.
- Malinauskas, A., Holze, R., 1998. UV-vis spectroelectrochemical detection of intermediate species in the electropolymerization of an aniline derivative. *Electrochim. Acta* 43, 2413–2422.
- Mascaro, L.H., Goncalves, D., Bulhoes, L.O.S., 2004. Electrocatalytic properties and electrochemical stability of polyaniline and polyaniline modified with platinum nanoparticles in formaldehyde medium. *Thin Solid Films* 461, 243–249.
- Motheo, A.J., Santos, J.R., Venancio, E.C., Mattoso, L.H.C., 1998. Influence of different types of acidic dopant on the electrodeposition and properties of polyaniline films. *Polymer* 39, 6977–6982.
- Neghmouche, N.S., Lanez, T., 2013. Calculation of diffusion coefficients and layer thickness for oxidation of the ferrocene using voltammetry technique. *Int. J. Chem. Stud.* 1, 28–32.
- Nekrasov, A.A., Ivanov, V.F., Vannikov, A.V., 2000. Analysis of the structure of polyaniline absorption spectra based on spectroelectrochemical data. *J. Electroanal. Chem.* 482, 11–17.
- Obaid, A.Y., El-Mossalamy, E.H., Al-Thabaiti, S.A., El-Hallag, I.S., Hermas, A.A., Asiri, A.M., 2014. Electrodeposition and characterization of polyaniline on stainless steel surface via cyclic, convolutive voltammetry and SEM in aqueous acidic solutions. *Int. J. Electrochem. Sci.* 9, 1003–1015.
- Park, Y.R., Doh, J.H., Shin, K., Seo, Y.S., Kim, Y.S., Kim, S.Y., Choi, W.K., Hong, Y.J., 2015. Solution-processed quantum dot light-emitting diodes with PANI: PSS hole-transport interlayers. *Org. Electron.* 19, 131–139.
- Reda, S.M., Al-Ghannam, S.M., 2012. Synthesis and electrical properties of polyaniline composite with silver nanoparticles. *Adv. Mater. Phys. Chem.* 2, 75–81.
- Sai-Anand, G., Gopalan, A.-I., Lee, K.-P., Venkatesan, S., Kang, B.-H., Lee, S.-W., Lee, J.-S., Qiao, Q., Kwon, D.-H., Kang, S.-W., 2015. A futuristic strategy to influence the solar cell performance using fixed and mobile dopants incorporated sulfonated polyaniline based buffer layer. *Sol. Energy Mater. Sol. Cells* 141, 275–290.
- Sonmezoglu, S., Akyurek, C., Akin, S., 2012. High-efficiency dye-sensitized solar cells using ferrocene-based electrolytes and natural photosensitizers. *J. Phys. D: Appl. Phys.* 45.
- Steim, R., Kogler, F.R., Brabec, C.J., 2010. Interface materials for organic solar cells. *J. Mater. Chem.* 20, 2499–2512.
- Subathira, A., Meyyappan, R.M., 2010. Electrodeposition of polyaniline on stainless steel and its role on corrosion prevention. *Natl. J. ChemBiosis* 1, 16–21.
- Taş, R., Gülen, M., Can, M., Sönmezoglu, S., 2016. Effects of solvent and copper-doping on polyaniline conducting polymer and its application as a counter electrode for efficient and cost-effective dye-sensitized solar cells. *Synth. Met.* 212, 75–83.
- Thompson, B.C., Frechet, J.M.J., 2008. Organic photovoltaics – polymer-fullerene composite solar cells. *Angew. Chem.: Int. Ed.* 47, 58–77.
- Wang, H.-z, Zhang, P., Zhang, W.-g, Yao, S.-w, 2012. Electrodeposition and characterization of polyaniline film. *Chem. Res. Chin. Univ.* 28, 133–136.
- Wang, S., Lu, S., Li, X., Zhang, X., He, S., He, T., 2013. Study of H<sub>2</sub>SO<sub>4</sub> concentration on properties of H<sub>2</sub>SO<sub>4</sub> doped polyaniline counter electrodes for dye-sensitized solar cells. *J. Power Sources* 242, 438–446.
- Winther-Jensen, B., MacFarlane, D.R., 2011. New generation, metal-free electrocatalysts for fuel cells, solar cells and water splitting. *Energy Environ. Sci.* 4, 2790–2798.
- Xia, Y.N., Wiesinger, J.M., Macdiarmid, A.G., Epstein, A.J., 1995. Camphorsulfonic acid fully doped polyaniline emeraldine salt – conformations in different solvents studied by an ultraviolet-visible near-infrared spectroscopic method. *Chem. Mater.* 7, 443–445.
- Yip, H.-L., Jen, A.K.Y., 2012. Recent advances in solution-processed interfacial materials for efficient and stable polymer solar cells. *Energy Environ. Sci.* 5, 5994–6011.
- Yusairie, M., Ruhani, I., Muhammad, F.Z., 2012. Electrodeposition and characterization of polyaniline films. In: *Proceedings of IEEE Symposium on Humanities Science and Engineering Research*.
- Zhang, L., Hou, B., Lang, Q., 2011. In situ UV-vis spectroelectrochemical studies on the copolymerization of diphenylamine and o-phenylenediamine. *Am. J. Anal. Chem.* 2, 182–193.